

000 001 002 003 004 005 006 007 008 009 010 011 012 013 014 015 016 017 018 019 020 021 022 023 024 025 026 027 028 029 030 031 032 033 034 035 036 037 038 039 040 041 042 043 044 045 046 047 048 049 050 051 052 053 TEMPORAL-AWARE ITERATIVE SPEECH MODEL FOR DEMENTIA DETECTION

Anonymous authors

Paper under double-blind review

ABSTRACT

Current acoustic markers for dementia detection often rely on static feature aggregation or error-prone linguistic transcription (ASR), thereby failing to capture the fine-grained, frame-to-frame temporal deterioration of articulatory motor control. To address this, we introduce TAI-Speech, an ASR-free framework that models speech deterioration as a continuous temporal trajectory analogous to physical motion. Our architecture introduces two key innovations: 1) Optical Flow-inspired Iterative Refinement: By treating spectrograms as sequential frames, this component uses a convolutional GRU to capture the fine-grained, frame-to-frame evolution of acoustic features; and 2) Cross-Modal Attention, which dynamically aligns spectral features with prosodic contours (pitch and pauses) to detect pathological mismatches. Experimental evaluation on the DementiaBank Corpus demonstrates that TAI-Speech achieves an AUC of 83.9% and Recall of 89.0%. Importantly, our model surpasses strong state-of-the-art baselines on AUC ROC, including fine-tuned Wav2Vec 2.0 (67.9%), Audio Spectrogram Transformers (74.8%), and CNNs (76.8%). These results confirm that explicitly modeling acoustic flow yields superior diagnostic sensitivity compared to latent linguistic representations or static classifiers, offering a privacy-preserving and computationally efficient solution for early cognitive screening.

1 INTRODUCTION

Dementia is a progressive neurodegenerative syndrome currently affecting an estimated 55 million people worldwide, with prevalence projected to rise sharply by 2050. It is marked by gradual decline in memory, language, and executive function, and Alzheimer’s disease remains the most common subtype (Ortiz-Perez et al. (2023),Pan et al. (2025),Agbavor & Liang (2022),Galanakis et al. (2025)). Early detection is critical for timely intervention and improved quality of life (Ortiz-Perez et al. (2023),Gkoumas et al. (2024)). Among the most promising non-invasive biomarkers are speech and language changes, which often appear during preclinical stages (Gkoumas et al. (2024),Agbavor & Liang (2022),Pan et al. (2025),Li et al. (2025),Kannoja et al. (2025),Yeung et al. (2021)).

Speech deterioration is closely tied to functional decline measured by Instrumental Activities of Daily Living (IADLs) abilities such as financial management, medication adherence, and complex communication (Fieo et al. (2014),Laurentiev et al. (2024),Fieo & Stern (2018)). Extended IADL (x-IADL) scales correlate strongly with language function, processing speed, and visuospatial ability (Fieo et al. (2014)). Despite extensive work analyzing speech or IADLs separately, current methods rarely model their temporal interdependence, even though language decline, commonly characterized as slowed speech, lexical retrieval failures, and reduced syntactic complexity, often precedes measurable IADL impairment (Yeung et al. (2021),Chen & Li (2024)).

We hypothesize that gradual, fine-grained deterioration of speech is a precursor to IADL impairment and can be captured by an architecture inspired by optical-flow estimation. Both problems require tracking continuous temporal changes via correspondence analysis and iterative refinement (Alfarano et al. (2024),Teed & Deng (2021)). Analogous to how optical flow estimates motion between video frames, our approach models the temporal evolution of spectrogram frames, allowing precise characterization of pauses, pitch variability, and other subtle acoustic patterns.

We present TAI-Speech, a deep learning framework that treats speech not as a static signal, but as a dynamic sequence of evolving spectrogram frames. Based on cross-modal research demonstrating

054 that physical articulatory motions and acoustic signals share a consistent temporal and structural
 055 correspondence (Zhao et al. (2018), Ephrat et al. (2018)), we adapt the Recurrent All-Pairs Field
 056 Transform (RAFT) paradigm (Alfarano et al. (2024), Teed & Deng (2021), Sui et al. (2022)) to audio
 057 analysis. Rather than estimating explicit motion vectors, we leverage RAFT’s iterative refinement
 058 to construct a temporally aware embedding that captures the “velocity” of spectral degradation. A
 059 convolutional GRU serves as the recurrent update module, iteratively refining these latent represen-
 060 tations, while cross-attention dynamically aligns acoustic features with prosodic cues. While our
 061 conceptual framework is motivated by the functional deterioration seen in IADLs, we empirically
 062 validate TAI-Speech as a detector of acoustic motor instability the upstream mechanistic failure that
 063 serves as a proximal biomarker for downstream functional decline. Evaluated on the DementiaBank
 064 corpus, our approach outperforms strong linguistic baselines, demonstrating that modeling these
 065 temporal dynamics offers a robust, ASR-free alternative for early detection.
 066

067 Our Contribution

068 • We adapted iterative-refinement priors from optical-flow modeling (Teed & Deng, 2021) to
 069 audio by treating non-stationary acoustic variation as continuous manifold evolution.
 070 • Propose a dual-stream ASR-free architecture with a temporal-consistency objective and
 071 cross-modal attention linking spectral and prosodic dynamics.
 072 • Establish a temporally regularized training framework that enforces physically grounded
 073 continuity in acoustic trajectories, enabling strong performance in low-resource clinical-
 074 speech settings without transcription.
 075

076 2 RELATED WORK

077 2.1 COMPUTATIONAL APPROACHES TO SPEECH BASED DEMENTIA DETECTION

078 Speech analysis has emerged as a non-invasive, cost-effective modality for early dementia diagnosis
 079 and monitoring (Ortiz-Perez et al. (2023); Agbavor & Liang (2022); Braun et al. (2024)). A corner-
 080 stone resource is the DementiaBank Corpus, which records subjects describing the “Cookie Theft”
 081 picture see Figure 1 to elicit lexical retrieval challenges and discourse impairments. Its deriva-
 082 tives, ADReSS and ADReSSo provide balanced demographics and higher acoustic quality, support-
 083 ing tasks such as Alzheimer’s disease classification, MMSE regression, and cognitive-decline pre-
 084 diction, with ADReSSo emphasizing speech-only input and ASR-generated transcripts (Luz et al.
 085 (2021)).
 086

087 Feature extraction spans acoustic (log-Mel spectrograms, MFCCs, energy contours, pauses, hes-
 088 itations) and linguistic (vocabulary richness, syntactic complexity, POS distributions, disfluency
 089 metrics) domains (Ortiz-Perez et al. (2023); Braun et al. (2024); Ilias & Askounis (2023); Woszczyk
 090 et al. (2024)). Deep models dominate: CNNs for audio, RNN/LSTM and Transformer variants (e.g.,
 091 BERT, RoBERTa, DeiT, GPT-3) for both acoustic and text representations (Pan et al. (2025); Braun
 092 et al. (2024); Meilán et al. (2014); König et al. (2018); Gong et al. (2021a)). Self-supervised models
 093 such as wav2vec 2.0 capture rich acoustic embeddings with strong downstream performance (Pan
 094 et al. (2025); Braun et al. (2024)).
 095

096 Multimodal fusion strategies integrate modalities through early feature concatenation, late decision-
 097 level aggregation, and cross-attention mechanisms that dynamically weight each modality. Although
 098 ASR errors can introduce noise, transcripts with relatively high Word Error Rates (WER) often
 099 perform on par with or better than manual transcriptions for dementia classification, suggesting that
 100 salient cognitive cues persist in noisy outputs (Pan et al. (2025); Shon et al. (2023)).
 101

102 2.2 CORRELATING SPEECH WITH FUNCTIONAL DECLINE

103 Loss of independence in Instrumental Activities of Daily Living (IADLs) is a defining clinical
 104 marker of dementia (Fieo et al. (2014); Liepelt-Scarfone et al. (2013)). Modern, technology-
 105 mediated IADLs such as online financial tasks or text messaging—offer even greater sensitivity
 106 for early Alzheimer’s detection (Benge et al. (2024)). Numerous studies report strong links between
 107 speech abilities and functional status: language deficits often precede measurable IADL impairment
 108 (Gkoumas et al. (2024); Yeung et al. (2021)).
 109

108
109
110
111
112
113
114
115
116
117
118
119
120
121
122
123
124
125
126
127
128

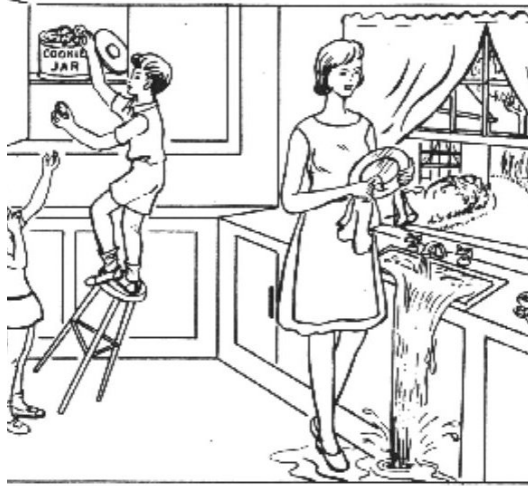


Figure 1: Cookie Theft picture

129 Automated speech and language analysis captures these associations objectively. Word-finding dif-
130 ficulty correlates with increased pause frequency and specific acoustic signatures (e.g., MFCC pat-
131 terns), while incoherence and perseveration manifest as degraded discourse structure and repeated
132 utterances measurable via cosine similarity. Reduced lexical diversity, simplified grammar, and
133 malformed verb phrases signal syntactic and semantic breakdown (Yeung et al. (2021)). Beyond
134 structured tasks, NLP methods applied to unstructured clinical narratives in EHRs extract indica-
135 tors of IADL/ADL impairment, enabling scalable integration of functional status into research and
136 clinical decision support (Laurentiev et al. (2024); Penfold et al. (2022)).

2.3 ITERATIVE REFINEMENT IN OPTICAL FLOW

137 Optical flow research has advanced from classical variational formulations to deep iterative refine-
138 ment. RAFT achieves state-of-the-art accuracy by maintaining high-resolution flow fields and lever-
139 aging multi-scale correlation volumes with a convolutional GRU for recurrent updates (Teed &
140 Deng (2021); Sui et al. (2022)). Follow-on architectures such as IRR and LiteFlowNet refine cost
141 volumes through shared-weight cascades and optimized objectives like RCELoss (Alfarano et al.
142 (2024); Hui et al. (2018)). These iterative principles, high-resolution correlation, recurrent updates,
143 and context preservation inform broader temporal modeling strategies and motivate cross-domain
144 applications beyond computer vision (Alfarano et al. (2024); Meßmer et al. (2025)).

2.4 THEORETICAL FRAME FOR TEMPORAL ANALYSIS

145 Speech is a fundamentally temporal information modality, where the state at a given moment is in-
146 trinsically linked to its context. Temporal aspects in audio, such as hesitation and pauses, speaking
147 rate, and word duration, serve as significant indicators of cognitive decline Xu et al. (2023). Demen-
148 tia recordings exhibit prolonged utterances and characteristic pause patterns, with manual transcripts
149 often marking these events explicitly (Ortiz-Perez et al. (2023),Pan et al. (2025),Braun et al. (2024)).
150 Acoustic representations such as log-Mel spectrograms, MFCCs, and eGeMAPS capture short-term
151 spectral and physiological voice dynamics (GOrtiz-Perez et al. (2023),Gong et al. (2021a),Corvitto
152 et al. (2024), Luz et al. (2021)).

153 Longitudinal analysis tracks language change across sessions via embedding similarity and related
154 metrics (Gkoumas et al. (2024),Braun et al. (2024)). Linguistic deficits, empty speech, circumlocu-
155 tion, repetition, poor grammar are temporal manifestations of cognitive decline (Chen & Li (2024)).
156 Extra-linguistic cues such as keystroke pauses in written text further complement audio evidence
157 (Gkoumas et al. (2024)).

162 Context-aware large language models can exploit preceding audio or text to predict next-sentence
 163 semantics or topic flow, enhancing downstream temporal reasoning (Shon et al. (2023),Bai et al.
 164 (2024)). Related techniques in audio-visual segmentation similarly rely on temporal consistency,
 165 where optical flow provides low-level motion signals for tasks like emotion recognition and lip-
 166 reading (Alfarano et al. (2024),Torabi & Nilchi (2014)). Temporal Enhancement Modules (TEM)
 167 extend these ideas by exchanging learnable context tokens across frames to strengthen inter-frame
 168 coherence (Geng & Gu (2025)).

169 2.5 CROSS-MODAL DYNAMIC COUPLING

170 Foundational work in The Sound of Pixels (Zhao et al. (2018)), sound of motion (Zhao et al. (2019))
 171 and visual speech recognition (Ephrat et al. (2018)) establishes that acoustic output is the causal
 172 result of physical motor dynamics. These studies demonstrate that while the mapping is not strictly
 173 bijective, the temporal derivatives of physical motion (e.g., lip velocity) are structurally preserved
 174 in the evolution of the acoustic manifold. This kinematic-acoustic coupling provides the theoretical
 175 justification for applying motion-tracking architectures specifically Optical Flow priors to purely
 176 acoustic time-series, as the velocity of spectral degradation serves as a proxy for the underlying
 177 articulatory drift.

178 3 METHODOLOGY

179 3.1 TASK AND DATASET

180 We evaluate our approach on spontaneous picture description, a standardized neurocognitive
 181 paradigm used to probe semantic memory and episodic retrieval (Mueller et al. (2018)). Participants
 182 describe the Cookie Theft line drawing (Lanzi et al. (2023)), producing naturalistic speech
 183 that reveals lexical retrieval difficulty, hesitations, and discourse-level impairments.

184 Experiments use the DementiaBank Corpus, the largest publicly available speech dataset for
 185 cognitive-impairment assessment. We focus on the clinically validated subsets comprising
 186 222 recordings from 89 healthy controls (HC) and 255 recordings from 168 participants with
 187 Alzheimer’s disease (AD), for a total of 477 audio samples. All recordings are accompanied by
 188 diagnostic annotations and are sampled at 16 kHz.

189 3.2 MODEL ARCHITECTURE

190 Our goal is to capture temporal markers of functional decline, particularly those linked to Instrumental
 191 Activities of Daily Living directly from raw speech. **TAI-Speech** integrates prosodic encodings,
 192 convolutional spectral processing, iterative temporal refinement, and sequence-level aggregation
 193 (Figure 2). The model is trained end-to-end with a joint objective combining cross-entropy
 194 classification and a temporal smoothness regularizer to enforce stability across successive frames.

195 3.3 FEATURE ENCODINGS

196 Raw speech $x(t)$ is first resampled and transformed using the short-time Fourier transform (STFT).
 197 A log-Mel spectrogram is computed:

$$200 S(m, n) = \log \left(\sum_k |X(k, n)|^2 H_m(k) \right), \quad (1)$$

201 where $X(k, n)$ is the STFT coefficient at frequency k and frame n , and H_m is the m -th Mel filter.
 202 Tabler 1 summaries the notation

203 Prosodic correlates relevant to IADL are explicitly extracted: (i) normalized pitch track $\tilde{p}(n)$, and
 204 (ii) pause probability $q(n)$ estimated from voice activity detection. These auxiliary encodings are
 205 fused into a joint representation:

$$206 z(n) = \phi(W_f[\tilde{p}(n), q(n)] + b_f), \quad (2)$$

207 where W_f and b_f are trainable parameters and $\phi(\cdot)$ is a non-linear activation.

216
217
218
219
220
221
222
223
224
225
226
227
228
229
230
231
232
233
234
235
236
237
238
239
240
241
242
243
244
245
246
247
248

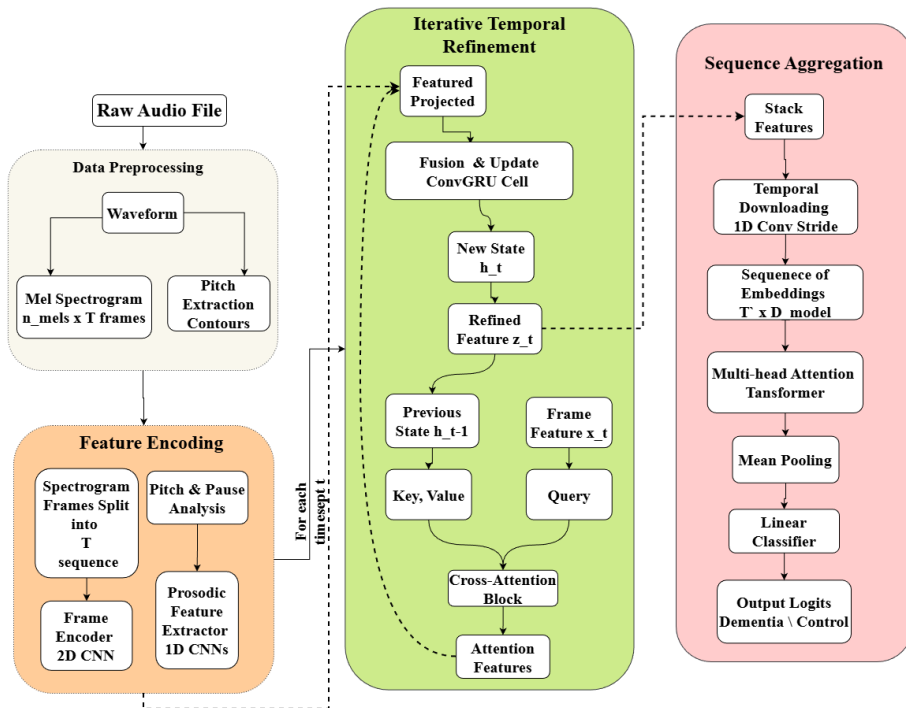


Figure 2: Architecture Model

Table 1: Summary of Notations and Their Meanings

Symbol	Meaning	Symbol	Meaning
$x(t)$	Raw speech waveform	$S(m, n)$	Log-Mel spectrogram value
$X(k, n)$	STFT coefficient	$H_m(k)$	m -th Mel filter
$\tilde{p}(n)$	Normalized pitch track	$q(n)$	Pause probability
$z(n)$	Prosodic feature vector	W_f, b_f	Trainable weight and bias
$\phi(\cdot)$	Non-linear activation	$h^{(l)}$	Local spectral embedding
Attn(Q,K,V)	Cross-modal attention	Q, K, V	Query, Key, Value matrices
r_t, u_t	Reset and update gates	H_t	Hidden state at time t
\tilde{H}_t	Candidate hidden state	\odot	Element-wise multiplication
$*$	Convolution operation	$\{h_1, \dots, h_T\}$	Sequence of embeddings
u_{cls}	Classification token	U	Transformer output
\hat{y}	Predicted probability	W_c, b_c	Classification layer params
L	Total training loss	L_{CE}	Cross-entropy loss
$\lambda_{cls}, \lambda_{temp}$	Regularization weights	$\ h_t - h_{t-1}\ _2^2$	Temporal consistency term

270 3.4 TEMPORAL REFINEMENT MODULES
271272 3.4.1 CROSS-ATTENTION CONTEXTUALIZATION
273274 The spectral encoder produces local embeddings $h^{(l)}$. To integrate prosodic factors, a cross-modal
275 attention module computes:

276
$$\text{Attn}(Q, K, V) = \text{softmax}\left(\frac{QK^\top}{\sqrt{d}}\right)V, \quad (3)$$

277

278 where queries Q are derived from spectro-temporal features, while keys and values come from $z(n)$.
279 This aligns acoustic features with temporal dynamics of pitch and pause, providing contextualized
280 embeddings.
281282 3.4.2 ITERATIVE UPDATE BLOCK
283284 To refine temporal representations, we employ a multi-scale ConvGRU. At each time step t , the
285 hidden state H_t is updated by:

286
$$r_t = \sigma(W_r * x_t + U_r * H_{t-1}), \quad (4)$$

287

288
$$u_t = \sigma(W_u * x_t + U_u * H_{t-1}), \quad (5)$$

289

290
$$\tilde{H}_t = \tanh(W * x_t + U * (r_t \odot H_{t-1})), \quad (6)$$

291

292
$$H_t = u_t \odot H_{t-1} + (1 - u_t) \odot \tilde{H}_t, \quad (7)$$

293

294 where $*$ denotes convolution and \odot elementwise multiplication. This iterative block progressively
295 corrects and stabilizes features across multiple scales, reflecting temporal organization in speech.
296297 3.5 SEQUENCE AGGREGATION AND CLASSIFICATION
298299 Downsampled embeddings $\{h_1, \dots, h_T\}$ are passed into a Transformer encoder augmented with a
300 classification token u_{cls} . The self-attention mechanism models higher-order dependencies:

301
$$U = \text{Transformer}([u_{\text{cls}}, h_1, \dots, h_T]). \quad (8)$$

302

303 The final classification is computed as:

304
$$\hat{y} = \text{softmax}(W_c u'_{\text{cls}} + b_c), \quad (9)$$

305

306 where u'_{cls} is the contextualized embedding.
307308 The training objective combines cross-entropy loss with a temporal consistency regularizer:
309

310
$$\mathcal{L} = \lambda_{\text{cls}} \mathcal{L}_{\text{CE}}(\hat{y}, y) + \lambda_{\text{temp}} \frac{1}{T-1} \sum_{t=2}^T \|h_t - h_{t-1}\|_2^2, \quad (10)$$

311

312 encouraging stability in temporal encodings while preserving discriminative capacity. While the first
313 term minimize standard cross-entropy error for classification, the second term temporal consistency
314 regularizer, penalizes the squared Euclidean distance between consecutive hidden states (h_t, h_{t-1}) to
315 enforce smooth latent evolution. This constraint ensures that learned features reflect the continuous
316 acoustic drift of physiological decline rather than overfitting to transient noise artifacts.
317318 4 EXPERIMENTAL SETUP
319320 4.1 EVALUATION PROTOCOL
321322 In order to guarantee a rigorous and unbiased evaluation of the proposed approach, we adopt a strat-
323 ified five-fold cross-validation (5-fold CV) protocol. This strategy preserves the original class dis-
324 tribution within each fold, a critical consideration when working with imbalanced clinical datasets.
325 The primary evaluation metric is the Area Under the Curve (AUC), which provides a robust mea-
326 sure of discriminative capability between dementia and healthy control groups. In addition, we
327 report secondary performance indicators, namely accuracy, precision, recall, and F1-score, thereby
328 offering a comprehensive assessment across multiple dimensions of classification performance.
329

324
325 **Algorithm 1:** TAI-Speech: Temporal–Acoustic–IADL Speech Classification

326 **Input:** Raw waveform $x(t)$;
327 ground-truth label y
328 **Output:** Predicted probability \hat{y}
329 # Preprocessing
330 Resample $x(t)$ and compute log-Mel spectrogram $S(m, n) = \log \sum_k |X(k, n)|^2 H_m(k)$
331 Extract normalized pitch $\tilde{p}(n)$ and pause probability $q(n)$
332 Fuse prosodic vector $z(n) = \phi(W_f[\tilde{p}(n), q(n)] + b_f)$
333 # Spectral Encoding
334 $h(l) \leftarrow$ Hierarchical convolutional encoder on $S(m, n)$
335 # Cross-Attention Contextualization
336 $h'(l) \leftarrow \text{Attn}(Q, K, V)$ with $Q = h(l)$;
 $K, V = z(n)$
337 # Iterative Temporal Refinement
338 **for** $t = 1$ **to** T **do**
339 $r_t = \sigma(W_r * x_t + U_r * H_{t-1})$
340 $u_t = \sigma(W_u * x_t + U_u * H_{t-1})$
341 $\tilde{H}_t = \tanh(W * x_t + U * (r_t \odot H_{t-1}))$
342 $H_t = u_t \odot H_{t-1} + (1 - u_t) \odot \tilde{H}_t$
343 # Sequence Aggregation and Classification
344 $U \leftarrow \text{Transformer}([u_{\text{cls}}, h'_1, \dots, h'_T])$
345 $\hat{y} \leftarrow \text{softmax}(W_c u'_{\text{cls}} + b_c)$
346 # Training Loss
347 $\mathcal{L} = \lambda_{\text{cls}} \mathcal{L}_{\text{CE}}(\hat{y}, y) + \lambda_{\text{temp}} \frac{1}{T-1} \sum_{t=2}^T \|h_t - h_{t-1}\|_2^2$
348 **return** \hat{y}

349
350
351 4.2 BASELINE SYSTEMS
352
353 To rigorously evaluate the proposed temporal modeling approach, we benchmark TAI-Speech
354 against three distinct architectural paradigms trained on the DementiaBank Corpus:
355

- 356 • Self-Supervised Foundation (Wav2Vec 2.0): We fine-tuned Wav2Vec 2.0 Baevski et al.
357 (2020) to evaluate the efficacy of latent linguistic representations pre-trained on healthy
358 speech for detecting pathological acoustic drift.
- 359 • Transformer-based (AST): We implemented the Audio Spectrogram Transformer Gong
360 et al. (2021b), which utilizes patch-based global self-attention, to assess whether global
361 context modeling suffices compared to frame-by-frame recurrent refinement.
- 362 • Static Convolutional (2D CNN): The 2D CNN Hershey et al. (2017) served as a time-
363 agnostic baseline to isolate the contribution of temporal dynamics versus static feature ag-
364 gregation.

365 Additionally, we reference recent multimodal state-of-the-art systems Braun et al. (2024); Pan et al.
366 (2025) to demonstrate the comparative efficacy of our ASR-free approach against text-dependent
367 architectures.

369
370 4.3 PROPOSED SYSTEM
371

372 **Algorithm.** Algorithm 1 presents the overall procedure of our proposed method. The TAI-Speech
373 framework refines acoustic representations of spontaneous speech to detect dementia-related func-
374 tional decline. The procedure can be summarized in three stages:

- 375 • **Acoustic Feature Encoding:** Raw audio $x(t)$ is converted into log-Mel spectrogram
376 frames $S(m, n)$. A hierarchical convolutional encoder extracts local spectral representa-
377 tions as initial feature maps.

- **Iterative Temporal Refinement:** Hidden states H_t are updated with a multi-scale ConvGRU to capture long-range temporal context. The prosodic characteristics, the normalized pitch $\tilde{p}(n)$ and the probability of pause $q(n)$, are fused using a cross-modal attention layer for richer temporal contextualization.
- **Sequence Aggregation and Classification:** Refined embeddings are downsampled and passed through a Transformer encoder with a learnable classification token u_{cls} . A final linear layer with softmax outputs the dementia vs. control prediction. Training employs a cross-entropy loss plus a temporal-smoothness regularizer to encourage frame-to-frame consistency.

388 4.4 TRAINING DETAILS

390 **Signal Processing and Feature Extraction.** Raw audio is resampled to 16 kHz. Log-Mel spectrograms are computed using an STFT with a window size (n_fft) of 2048, a hop length of 512, and 64 Mel filterbanks spanning 0–8000 Hz. Prosodic features are extracted using `librosa.piptrack`, with pitch constrained to 75–400 Hz. Voice activity detection is performed using an energy-based method with 25 ms frames and a normalized energy threshold of 0.01 to generate pause-probability sequences.

396 **Training Configuration.** All models are trained under a unified protocol for comparability. Optimization uses AdamW with a batch size of 4, a maximum of 200 epochs, and an initial learning rate of 1×10^{-5} . Early stopping with a patience of 10 epochs based on validation AUC is applied to mitigate overfitting. Class imbalance is handled via a `WeightedRandomSampler` to maintain uniform class representation per batch. Training is conducted on a single NVIDIA RTX A4000 GPU (32 GB).

403 5 RESULTS AND DISCUSSION

405 This section presents the performance of our proposed architecture, contextualizes the findings by comparing them against established baseline models, and discusses the broader implications of our 406 results, with a specific focus on how the model’s design relates to the detection of functional decline.

409 5.1 QUANTITATIVE PERFORMANCE ANALYSIS

411 The proposed model was rigorously evaluated using a 5-fold cross-validation protocol. The primary 412 metric for assessing the model’s ability to discriminate between dementia and healthy control classes 413 was the Area Under the Curve (AUC), with Accuracy (ACC), Recall (REC), and F1-score also 414 reported for a comprehensive analysis.

415 As summarized in Table 2, our proposed architecture achieved a high level of discriminative 416 performance, yielding a test AUC of 0.839. The model obtained an accuracy of 80.55%, recall of 0.890, 417 and an F1-score of 0.813.

419 420 **Table 2: The Result (%) of our Model**

421 System	AUC	ACC	REC	F1-score
422 Our Model	83.9	0.81	0.890	0.813

423 For evaluation, we benchmarked our system against previously reported baseline models, as well as 424 Transformer-based acoustic approaches that analyze transcribed speech.

426 The TAI-Speech architecture achieved an AUC of 0.839, an accuracy of 80.55%, a recall of 89.0%, 427 and an F1-score of 0.813. These results represent a significant improvement over purely linguistic 428 baselines. When benchmarked against state-of-the-art systems in table 3, our model demonstrates 429 good performance across all evaluation metrics. The 8% improvement in AUC over Braun et al. 430 (2024).’s pause-infused text model (77.2%) and competitive performance against Pan et al. (2025) 431 attention-based multimodal system (82.56% accuracy) underscore the efficacy of our temporatively 432 on acoustic signals without requiring error-prone ASR transcription or linguistic feature extraction.

432
433
434
435
436
437
438
439

Table 3: Performance comparison between the proposed model with other modalities

System	Modality	AUC (%)	Acc (%)	Recall	F1-score
Pan et al. (2019)	Linguistic	–	70.83	0.71	0.70
Pan et al. (2025)	Multimodal	–	82.56	0.83	0.83
Braun et al. (2024)	Multimodal	77.2	–	–	–
Our Model	Acoustic-Temporal	83.9	80.55	0.89	0.83

While systems incorporating ASR features achieve the highest AUC and accuracy, our purely acoustic model obtains the highest recall. It is notable that TAI-Speech achieves this level of performance without relying on a linguistic pipeline. This suggests that the temporal dynamics encoded within the acoustic signal contain sufficient information for effective dementia classification. This single-modality approach may offer advantages in robustness and simplicity, as it avoids potential cascading errors from ASR systems, which can struggle with the atypical speech patterns often present in clinical populations. The results indicate that direct modeling of speech dynamics is a viable and powerful alternative to multimodal approaches that require transcription.

Quantitative Analysis of Baselines. As shown in Table 4, TAI-SPEECH achieves the best overall performance (AUC 0.83, Recall 0.89), validating the value of temporally regularized acoustic modeling. Foundation models like Wav2Vec 2.0 underperform (AUC 0.679, Acc 0.565), likely due to pre-training on healthy speech that biases toward linguistic clarity, filtering out pathological drift signals critical in dementia. AST (AUC 0.748) highlights the limitations of patch-based attention: global spectrogram partitioning disrupts the continuity needed to track motor decline. ResNet50 (AUC 0.768) performs better by capturing local spectral texture. The 6.2% AUC gain from TAI-Speech over ResNet confirms the necessity of modeling acoustic flow frame-to-frame evolution as opposed to static aggregation. Clinically, the high Recall (0.89) positions TAI-Speech as a reliable screening tool, minimizing false negatives in early-stage detection.

5.2 DISCUSSION

Architectural Inductive Bias. The performance gap between TAI-Speech (AUC 0.839) and the baselines provides empirical validation for the acoustic flow hypothesis. While the Audio Spectrogram Transformer (AUC 0.748) captures global context, its patch-based processing fragments the continuous temporal trajectory required to detect fine-grained motor degradation. Similarly, the static CNN baseline (AUC 0.768) captures spectral texture but misses the velocity of decline. By adapting the Iterative Refinement mechanism from optical flow, TAI-Speech preserves the strict frame-to-frame continuity of the signal, confirming that a strong temporal inductive bias is more diagnostically relevant than global self-attention for non-stationary pathological signals.

Limitations of Linguistic Pre-training. The inferior performance of the fine-tuned Wav2Vec 2.0 baseline (AUC 0.679) highlights the risks of using foundation models pre-trained on healthy speech for pathology detection. These models optimize linguistic reconstruction, effectively treating pathological dysfluencies (e.g., slurring, tremors) as noise to be filtered. In contrast, TAI-Speech’s ASR-free design explicitly models these mechanical degradations, aligning with the Source-Filter theory where dementia manifests in the instability of the articulatory filter rather than the linguistic source.

Proximal Biomarkers of Functional Decline. Although direct IADL scores were not modeled, the high recall (0.89) indicates strong sensitivity to the proximal biomarkers of functional impairment. The Cross-Modal Attention mechanism successfully identifies pathological mismatches such

486 as silence aligned with rising pitch which serve as interpretable acoustic correlates of the executive
 487 dysfunction that precedes downstream IADL failure.
 488

489 **LIMITATIONS AND FUTURE DIRECTIONS**
 490

491 Despite promising results, this study has several limitations. The findings are based on a constrained
 492 dataset from a single linguistic and cultural context, which may limit their generalizability. The
 493 cross-sectional nature of the data also precludes any assessment of the model’s sensitivity to lon-
 494 gitudinal disease progression. Furthermore, the absence of direct IADL measurements restricts the
 495 empirical validation of our model’s relevance to functional decline. The model’s performance on
 496 mild cognitive impairment (MCI) also remains an open question for future investigation.
 497

498 Future work should aim to validate these findings on larger, more diverse, and longitudinal corpora.
 499 Incorporating patient IADL scores as an explicit modeling target could provide a more direct method
 500 for detecting functional decline. Exploring multimodal fusion, which would combine the temporal
 501 acoustic features from TAI-Speech with semantic embeddings from large language models, may
 502 also lead to improved robustness and performance. Finally, longitudinal studies are necessary to
 503 determine if changes in the model’s output correlate with cognitive trajectories over time, potentially
 504 enabling the use of personalized baselines for early detection.
 505

506 **6 CONCLUSION**
 507

508 We present TAI-SPEECH, a framework that reconceptualizes dementia detection as modeling the
 509 continuous dynamics of speech rather than relying on static acoustic categorization. By adapting
 510 the iterative refinement mechanism from optical flow, the model captures frame-to-frame acous-
 511 tic–prosodic evolution without requiring ASR. Our approach surpasses strong baselines including
 512 fine-tuned Wav2Vec 2.0, AST, and CNNs, achieving an AUC of 0.83 and a recall of 0.89. These
 513 findings indicate that recurrent refinement of acoustic flow provides greater diagnostic sensitivity
 514 than methods based on latent linguistic features or global patch-based attention. The ASR-free for-
 515 mulation also mitigates transcription errors and reduces computational and privacy burdens, making
 516 it suitable for clinical screening. Our results support acoustic motor instability as a reliable proximal
 517 biomarker, consistent with motor-control accounts of cognitive decline. Future work will validate
 518 this link using longitudinal datasets with functional impairment (IADL) measures and extend the
 519 framework to multilingual speech to assess cross-lingual generalization.
 520

521 **ACKNOWLEDGMENTS**
 522

523 The authors acknowledge the use of a Large Language Model (LLM) to assist in the editing and
 524 refinement of this manuscript. The LLM was utilized to improve grammar, clarity, and conciseness.
 525 All conceptual ideas, experimental design, analysis, and conclusions presented in this paper are the
 526 original work of the authors.
 527

528 **REFERENCES**
 529

530 F. Agbavor and H. Liang. Predicting dementia from spontaneous speech using large language mod-
 531 els. *PLOS Digital Health*, 1(12):e0000168, December 2022. doi: 10.1371/journal.pdig.0000168.
 532 A. Alfarano, L. Maiano, L. Papa, and I. Amerini. Estimating optical flow: A comprehensive review
 533 of the state of the art. *Computer Vision and Image Understanding*, 249:104160, December 2024.
 534 doi: 10.1016/j.cviu.2024.104160.
 535 Alexei Baevski, Henry Zhou, Abdelrahman Mohamed, and Michael Auli. wav2vec 2.0: a framework
 536 for self-supervised learning of speech representations. In *Proceedings of the 34th International
 537 Conference on Neural Information Processing Systems*, NIPS ’20, Red Hook, NY, USA, 2020.
 538 Curran Associates Inc. ISBN 9781713829546.
 539 Y. Bai et al. Seed-asr: Understanding diverse speech and contexts with llm-based speech recognition.
arXiv, July 2024. doi: 10.48550/arXiv.2407.04675.

540 J. F. Benge, D. A. González, A. Ali, N. Chandna, N. Rana, A. M. Kiselica, and M. K. Scullin.
 541 Technology-based instrumental activities of daily living in persons with alzheimer's disease and
 542 related disorders. *Alzheimer's & Dementia: Diagnosis, Assessment & Disease Monitoring*, 16
 543 (4):e70022, 2024. doi: 10.1002/dad2.70022.

544 F. Braun et al. Infusing acoustic pause context into text-based dementia assessment. *arXiv*, August
 545 2024. doi: 10.48550/arXiv.2408.15188.

547 C.-P. Chen and J.-L. Li. Profiling patient transcript using large language model reasoning aug-
 548 mentation for alzheimer's disease detection. In *46th Annual International Conference of*
 549 *the IEEE Engineering in Medicine and Biology Society (EMBC)*, pp. 1–4, July 2024. doi:
 550 10.1109/EMBC53108.2024.10782161.

551 L. Corvitto, L. Faiella, C. Napoli, A. Puglisi, and S. Russo. Speech and language impairment detec-
 552 tion by means of ai-driven audio-based techniques. In *Proceedings of the International Confer-
 553 ence on Advanced Intelligent Systems for Sustainable Development (AI2SD)*. Springer, 2024. doi:
 554 10.1007/978-3-031-52388-5_41.

555 Ariel Ephrat, Inbar Mosseri, Oran Lang, Tali Dekel, Kevin Wilson, Avinatan Hassidim, William T
 556 Freeman, and Michael Rubinstein. Looking to listen at the cocktail party: a speaker-independent
 557 audio-visual model for speech separation. *ACM Transactions on Graphics (TOG)*, 37(4):1–11,
 558 2018.

560 R. Fieo and Y. Stern. Increasing the sensitivity of functional status assessment in the preclinical
 561 range (normal to mild cognitive impairment): Exploring the iadl-extended approach. *Dement
 562 Geriatr Cogn Disord*, 45(5–6):282–289, 2018. doi: 10.1159/000487632.

563 R. Fieo, J. J. Manly, N. Schupf, and Y. Stern. Functional status in the young–old: Establishing a
 564 working prototype of an extended-instrumental activities of daily living scale. *J Gerontol A Biol
 565 Sci Med Sci*, 69(6):766–772, June 2014. doi: 10.1093/gerona/glt167.

566 I. Galanakis, R. F. Soldatos, N. Karanikolas, A. Voulodimos, I. Voyatzis, and M. Samarakou. En-
 567 hancing the prediction of episodes of aggression in patients with dementia using audio-based
 568 detection: A multimodal late fusion approach with a meta-classifier. *Applied Sciences*, 15(10):
 569 5351, May 2025. doi: 10.3390/app15105351.

571 Qian Geng and Xiaoguang Gu. Decoding audio related region with temporal and structural enhance-
 572 ment for audio visual segmentation. *Digital Signal Processing*, 165:105302, October 2025. doi:
 573 10.1016/j.dsp.2025.105302.

574 D. Gkoumas et al. A longitudinal multi-modal dataset for dementia monitoring and diagno-
 575 sis. *Language Resources & Evaluation*, 58(3):883–902, September 2024. doi: 10.1007/
 576 s10579-023-09718-4.

577 Yuan Gong, Yu-An Chung, and James Glass. Ast: Audio spectrogram transformer. *arXiv*, July
 578 2021a. doi: 10.48550/arXiv.2104.01778.

580 Yuan Gong, Yu-An Chung, and James Glass. Ast: Audio spectrogram transformer. In *Interspeech
 581 2021*, pp. 571–575, 2021b. doi: 10.21437/Interspeech.2021-698.

582 Shawn Hershey, Sourish Chaudhuri, Daniel P. W. Ellis, Jort F. Gemmeke, Aren Jansen, Chan-
 583 ning Moore, Manoj Plakal, Devin Platt, Rif A. Saurous, Bryan Seybold, Malcolm Slaney,
 584 Ron Weiss, and Kevin Wilson. Cnn architectures for large-scale audio classification. In *Int-
 585 ernational Conference on Acoustics, Speech and Signal Processing (ICASSP)*. 2017. URL
 586 <https://arxiv.org/abs/1609.09430>.

588 Tak-Wai Hui, Xiaou Tang, and Chen Change Loy. Liteflownet: A lightweight convolutional neural
 589 network for optical flow estimation. In *2018 IEEE/CVF Conference on Computer Vision and
 590 Pattern Recognition (CVPR)*, pp. 8981–8989, Salt Lake City, UT, USA, June 2018. IEEE. doi:
 591 10.1109/CVPR.2018.00936.

592 L. Ilias and D. Askounis. Context-aware attention layers coupled with optimal transport domain
 593 adaptation and multimodal fusion methods for recognizing dementia from spontaneous speech.
Knowledge-Based Systems, 277:110834, 2023. doi: 10.1016/j.knosys.2023.110834.

594 S. Kannoja et al. Dementia detection using multi-modal methods on audio data. *arXiv*, July 2025.
 595 doi: 10.48550/arXiv.2501.00465.
 596

597 A. König, N. Linz, J. Tröger, M. Wolters, J. Alexandersson, and P. Robert. Fully automatic speech-
 598 based analysis of the semantic verbal fluency task. *Dementia and Geriatric Cognitive Disorders*,
 599 45(3-4):198–209, 2018. doi: 10.1159/000487852.

600 A. M. Lanzi, A. K. Saylor, D. Fromm, H. Liu, B. MacWhinney, and M. L. Cohen. Dementiabank:
 601 Theoretical rationale, protocol, and illustrative analyses. *American Journal of Speech-Language
 602 Pathology*, 32(2):426–438, March 2023. doi: 10.1044/2022_AJSLP-22-00281.
 603

604 J. Laurentiev et al. Identifying functional status impairment in people living with dementia through
 605 natural language processing of clinical documents: Cross-sectional study. *J Med Internet Res*, 26:
 606 e47739, February 2024. doi: 10.2196/47739.

607 Y. Li et al. Machine learning-driven speech biomarker analysis: A novel approach for detecting
 608 cognitive decline in older adults. *Alzheimers Dement*, 20(Suppl 2):e089668, January 2025. doi:
 609 10.1002/alz.089668.
 610

611 I. Liepelt-Scarfone, M. Fruhmann Berger, D. Prakash, I. Csoti, S. Gräber, W. Maetzler, and D. Berg.
 612 Clinical characteristics with an impact on adl functions of pd patients with cognitive impairment
 613 indicative of dementia. *PLOS ONE*, 8(12):e82902, 2013. doi: 10.1371/journal.pone.0082902.

614 S. Luz, F. Haider, S. de la Fuente, D. Fromm, and B. MacWhinney. Detecting cognitive decline using
 615 speech only: The adresso challenge. In *Proceedings of the Annual Conference of the International
 616 Speech Communication Association (INTERSPEECH)*, volume 6, pp. 4211–4215, 2021.
 617

618 J. J. G. Meilán, F. Martínez-Sánchez, J. Carro, D. E. López, L. Millian-Morell, and J. M. Arana.
 619 Speech in alzheimer’s disease: Can temporal and acoustic parameters discriminate dementia?
 620 *Dementia and Geriatric Cognitive Disorders*, 37(5-6):327–334, 2014. doi: 10.1159/000356726.

621 Liane-Marina Meßmer, Patrizia Held, Alexander Bejan, Christophe Kunze, and Christoph Reich.
 622 Designing a dementia caregiver-centered recommendation and context-aware ai media analyti-
 623 cal application: A comprehensive system requirements analysis. *International Journal of Hu-
 624 man–Computer Interaction*, 41(7):3974–3993, 2025. doi: 10.1080/10447318.2024.2344913.
 625

626 K. D. Mueller, B. Hermann, J. Mecollari, and L. S. Turkstra. Connected speech and language
 627 in mild cognitive impairment and alzheimer’s disease: A review of picture description tasks.
 628 *Journal of Clinical and Experimental Neuropsychology*, 40(9):917–939, November 2018. doi:
 629 10.1080/13803395.2018.1446513.

630 D. Ortiz-Perez, P. Ruiz-Ponce, D. Tomás, J. Garcia-Rodriguez, M. F. Vizcaya-Moreno, and M. Leo.
 631 A deep learning-based multimodal architecture to predict signs of dementia. *Neurocomputing*,
 632 548:126413, 2023. doi: 10.1016/j.neucom.2023.126413.

633 Y. Pan, B. Mirheidari, M. Reuber, A. Venneri, D. Blackburn, and H. Christensen. Automatic hierar-
 634 chical attention neural network for detecting ad. In *Proc. Interspeech*, pp. 4105–4109, 2019. doi:
 635 10.21437/Interspeech.2019-1799.
 636

637 Y. Pan, B. Mirheidari, D. Blackburn, and H. Christensen. A two-step attention-based feature combi-
 638 nation cross-attention system for speech-based dementia detection. *IEEE Transactions on Audio,
 639 Speech and Language Processing*, 33:896–907, 2025. doi: 10.1109/TASLPRO.2025.3533363.

640 R. B. Penfold, D. S. Carrell, D. J. Cronkite, C. Pabiniak, T. Dodd, A. M. H. Glass, E. John-
 641 son, E. Thompson, H. M. Arrighi, and P. E. Stang. Development of a machine learning
 642 model to predict mild cognitive impairment using natural language processing in the absence
 643 of screening. *BMC Medical Informatics and Decision Making*, 22(1):129, May 2022. doi:
 644 10.1186/s12911-022-01864-z.
 645

646 Suwon Shon, Kwangyoun Kim, Prashant Sridhar, Yi-Te Hsu, Shinji Watanabe, and Karen Livescu.
 647 Generative context-aware fine-tuning of self-supervised speech models. *arXiv*, December 2023.
 doi: 10.48550/arXiv.2312.09895.

648 X. Sui et al. Craft: Cross-attentional flow transformer for robust optical flow. In *2022 IEEE/CVF*
 649 *Conference on Computer Vision and Pattern Recognition (CVPR)*, pp. 17581–17590, New Or-
 650 leans, LA, USA, June 2022. IEEE. doi: 10.1109/CVPR52688.2022.01708.

651

652 Z. Teed and J. Deng. Raft: Recurrent all-pairs field transforms for optical flow (extended abstract).
 653 In *Proceedings of the Thirtieth International Joint Conference on Artificial Intelligence*, pp. 4839–
 654 4843, Montreal, Canada, 2021. doi: 10.24963/ijcai.2021/662.

655

656 B. Torabi and A. R. Naghsh Nilchi. Automatic speech segmentation based on audio and optical
 657 flow visual classification. *International Journal of Image, Graphics and Signal Processing*, 6
 658 (11):43–49, October 2014. doi: 10.5815/ijigsp.2014.11.06.

659

660 D. Woszczyk, R. Aloufi, and S. Demetriou. Prosody-driven privacy-preserving dementia detection.
arXiv, July 2024. doi: 10.48550/arXiv.2407.03470.

661

662 Yurui Xu, Hang Su, Guijin Ma, and Xiaorui Liu. A novel dual-modal emotion recognition algorithm
 663 with fusing hybrid features of audio signal and speech context. *Complex & Intelligent Systems*, 9
 664 (1):951–963, February 2023. doi: 10.1007/s40747-022-00841-3.

665

666 A. Yeung et al. Correlating natural language processing and automated speech analysis with
 667 clinician assessment to quantify speech-language changes in mild cognitive impairment and
 668 alzheimer’s dementia. *Alzheimers Research & Therapy*, 13(1):109, June 2021. doi: 10.1186/s13195-021-00848-x.

669

670 Hang Zhao, Chuang Gan, Andrew Rouditchenko, Carl Vondrick, Josh McDermott, and Antonio
 671 Torralba. The sound of pixels. In *Proceedings of the European conference on computer vision*
(ECCV), pp. 570–586, 2018.

672

673 Hang Zhao, Chuang Gan, Wei-Chiu Ma, and Antonio Torralba. The sound of motions. In *Proceed-
 674 ings of the IEEE/CVF International Conference on Computer Vision*, pp. 1735–1744, 2019.

675

676

677

678

679

680

681

682

683

684

685

686

687

688

689

690

691

692

693

694

695

696

697

698

699

700

701